Available online at www.sciencedirect.com
ScienceDirect
Nuclear Instruments and Methods in Physics Research A 565 (2006) 855–860
NUCLEAR INSTRUMENTS & METHODS IN PHYSICS RESEARCH Section A
www.elsevier.com/locate/nima

Measurement of synchrotron radiation spectra using combined attenuation method and regularized inversion

Yonghua Du[a,c], Yanfei Wang[b], Wei Hua[a,c], Yuying Huang[a], Tiandou Hu[a,*]

[a]Institute of High Energy Physics, Chinese Academy of Sciences, Beijing 100049, China
[b]Institute of Remote Sensing Applications, Chinese Academy of Sciences, Beijing 100101, China
[c]Graduate University of Chinese Academy of Sciences, Beijing 100049, China

Received 21 March 2006; received in revised form 13 May 2006; accepted 13 May 2006
Available online 19 June 2006

Abstract

A method of measuring energy spectrum of synchrotron radiation (SR) based on attenuation is described in this paper. Tikhonov regularized method is applied to reconstruct the spectral distribution of SR. The feasibility of the method is studied in detail by using a hypothetical SR spectrum. The applied results of the spectrum of 4W1B beamline in BSRF (Beijing Synchrotron Radiation Facility) are shown.

PACS: 02.30.Zz; 41.50.+h; 07.85.Fv; 41.60.Ap; 07.85.Qe

Keywords: Synchrotron radiation; Tikhonov regularization method; Numerical inversion of Laplace transform; X-ray attenuation

1. Introduction

Since synchrotron radiation (SR) was first observed in 1947, it has been applied to many fields due to its good characters. One of the important characters is that the spectrum of SR source can be accurately calculated. So we often get the SR spectrum by theoretical calculation instead of experimental measurement. But, in reality, the feasibility of calculation is affected by many factors, for example, fluctuations of the parameter of insertion devices and the electron orbit, the change of acceptance angle. On the other hand, usually we are interested in the spectral distribution at the samples. The spectrum will be changed when the light transmit some optical elements in the beamline. Due to the above reasons, the experimental measurement of spectrum of SR is important in practice.

Some methods, such as monochromatization, detector with energy resolution and attenuation filter, have been developed to measure X-ray spectrum. But each of these methods has shortcomings of itself. For monochromatization method, the energy range of monochromator is limited and the real diffraction efficiency of the crystal is hard to confirm, which makes an exact calculation unfeasible. Another usual method is to measure directly by solid detector with energy resolution. In order to avoid the detector from being saturated, some kind of scatterer is always needed. This method overcomes the problem of energy limitation but complex scattering problem and the detector response have to be taken into account.

Attenuation filter is a simple method in experiment. But how to reconstruct the real spectrum is very difficult because it is faced with an ill-posed problem. The earliest method was an analytical approach using a Laplace transformation for representing the X-ray spectral distributions in a function form [1]. Later various techniques were developed [2–8], however, the computational results of those methods are not satisfying. Tikhonov regularization method, which has been applied successfully in a lot of fields such as signal and image processing [9] and Laplace transform [10]. It is a powerful tool to solve the operator equations off the first kind. In this paper the experimental method based on attenuation filter is improved and

*Corresponding author.
E-mail address: hutd@mail.ihep.ac.cn (T. Hu).

0168-9002/$ - see front matter © 2006 Elsevier B.V. All rights reserved.
doi:10.1016/j.nima.2006.05.169

Tikhonov regularization method is used to rebuild the spectrum of SR with enough accuracy.

2. Experiment method and mathematical model

2.1. Experimental geometry and components

The usual X-ray attenuation experiments were done by adding separated filtrations with different thickness in the light path. It is hard to reconstruct the spectral distribution accurately because only a few discrete data can be collected by this method. In order to obtain enough data easily, we adopt a wedged filtration. The filtration was driven by a step motor and at the same time its thickness was changed.

Details of the experimental setup are shown in Fig. 1. Experiments were done at 4W1B beamline in Beijing Synchrotron Radiation Facility (BSRF). SR is extracted at the straight section of 4W1 of the BSRF with an electromagnetic wiggler. The 4W1 wiggler is a single period wavelength shifter with magnetic period length 1.36 m, peak field of 1.8 T, and a gap 66 mm. There are two Be windows with 250 μm and an Al windows with 260 μm in the beamline. The slit was used to confine the incident X-ray to 0.1 mm × 1 mm. Two ion chambers filled with Ar are used to measure the intensity of SR. The first ion chamber was used to monitor of the intensity of incoming beam and the second one to record the transmitted intensity. The experimental curve is shown in Fig. 2.

2.2. Basic equations

When SR with spectrum distribution $f(E)$ traverses the filtration, the intensity is attenuated. The signal obtained by second ion chamber is

$$I(d) = a\int_{E_0}^{E_1} f(E)\,\mathrm{e}^{-\mu(E)d} E[1-\mathrm{e}^{-\mu_g(E)D}]\,\mathrm{d}E \quad (1)$$

where E is the energy of the light, $\mu_g(E)$ is the absorption coefficient of the gas filled in the chamber, D is the length

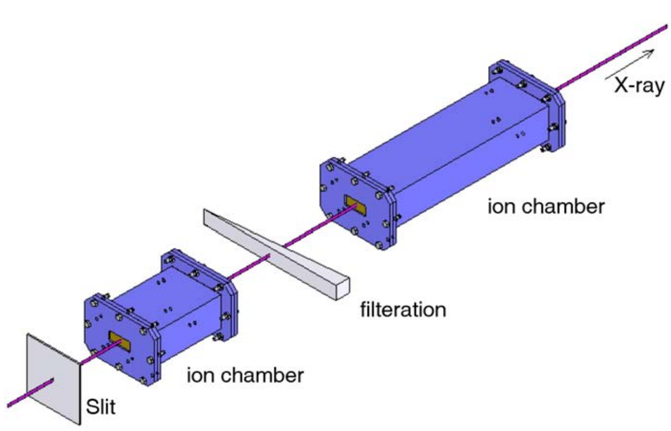

Fig. 1. Outline of the experimental setup. The slit was used to limit the incident X-ray to 0.1 mm (H) × 1 mm (V).

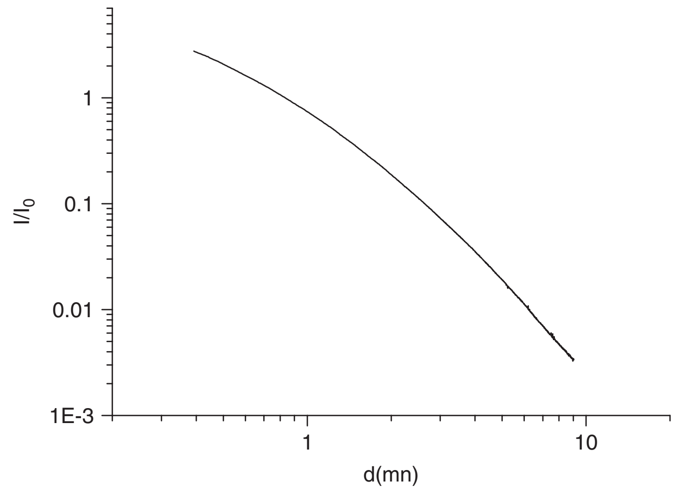

Fig. 2. Experiment curve. The material of the attenuation is Al.

of the ion chamber, E_0 and E_1 are the minimum and maximum photon energy of the incident light, respectively. Here, $a = Gq/\varepsilon_{\mathrm{ion}}$. G is the gain of the amplifier, q is the electron charge, $\varepsilon_{\mathrm{ion}}$ is the ionization energy of the gas filled in the chamber.

Considering the wedged filtration and the width of the beam, Eq. (1) has to be corrected

$$I(d) = a\int_{E_0}^{E_1} \frac{f(E)[1-\mathrm{e}^{-\mu(E)w\tan(\theta)}]}{\mu(E)w\tan(\theta)} \times E[1-\mathrm{e}^{-\mu_g(E)D}]\,\mathrm{e}^{-\mu(E)d}\,\mathrm{d}E \quad (2)$$

where w is the width of the light, θ is the apex angle of the filtration.

By variable replacement, Eq. (2) can be written as

$$I(d) = a\int_{\mu_0}^{\mu_1} g(\mu)\,\mathrm{e}^{-\mu d}\,\mathrm{d}\mu \quad (3)$$

where

$$g(\mu) = \frac{f[E(\mu)]E(\mu)\,\mathrm{e}^{-\mu_g E(\mu) D}[1-\mathrm{e}^{-\mu w\tan(\theta)}]}{\mu w\tan(\theta)}\frac{\mathrm{d}E}{\mathrm{d}\mu}.$$

Eq. (3) is a bounded Laplace transform for our detection system. Rewriting Eq. (3) in discrete form yields $y = Ax$. Where y and x are column vectors with the dimensions of m and n, respectively, and so A is an $m * n$ matrix. These are defined as

$$y = \begin{pmatrix} I(d_1) \\ \vdots \\ I(d_m) \end{pmatrix}, \quad x = \begin{pmatrix} g(\mu_1) \\ \vdots \\ g(\mu_m) \end{pmatrix},$$

$$A = a \triangle \mu \begin{pmatrix} \mathrm{e}^{-\mu_1 d_1} & \dots & \mathrm{e}^{-\mu_n d_1} \\ \vdots & \vdots & \vdots \\ \mathrm{e}^{-\mu_1 d_n} & \dots & \mathrm{e}^{-\mu_n d_n} \end{pmatrix}. \quad (4)$$

3. Regularized solution methods

Since the Laplace equation is a special integral equation of the first kind, hence the ill-posed nature inherits. This means even if a least-squares error solution exists, which may oscillate severely with the perturbation of the observation. Therefore, some kind of regularization technique must be involved to suppress the ill-posed characteristic [9,10]. Let us formulate the regularization in abstract normed space

$$(Lg)(\mu) = I(d). \tag{5}$$

We consider solve the unconstrained minimization problem

$$\|Lg - I\|^2_{L_2} + \alpha\|g\|^2_{W^1_2} \to \text{minimization} \tag{6}$$

where $\|\bullet\|$ is a normed space in Sobolev space, which means the function g is continuous and differentiable with the bounded norms of itself and its generalized derivatives in L_2. α is the so-called regularization parameter which is greater than zero.

Assume that the variation of g is flat near the boundary of the integral interval $[\mu_0, \mu_1]$. So, the derivatives of g are zeros at the boundary of $[\mu_0, \mu_1]$. Now by solution of Eq. (6), we obtain the following integro-differential equation with boundary condition [9]

$$\alpha[g''(r) - g(r)] - \int_{\mu_0}^{\mu_1} \bar{k}(\mu, v) g(v)\,\mathrm{d}v = \bar{I}(d) \tag{7}$$

$$g'(\mu_0) = 0, \quad g'(\mu_1) = 0 \tag{8}$$

where

$$\bar{k}(\mu, v) = \int_{\mu_0}^{\mu_1} k(\mu, d) k(v, d)\,\mathrm{d}d$$

$$\bar{I}(d) = -\int_{\mu_0}^{\mu_1} k(\mu, d) I(d)\,\mathrm{d}d$$

$$k(\mu, d) = a\,\mathrm{e}^{-\mu d}.$$

Eqs. (7)–(8) are the regularized form and can be used for the solution of g. By collocation, we have

$$L^* Lg + \alpha Hg = L^* I \tag{9}$$

where L^* is the adjoint operator of L, H is a scale operator which is in the form of a triangular matrix in finite space

$$H = \begin{pmatrix} 1+1/h^2 & -1/h^2 & & & \\ -1/h^2 & 1+2/h^2 & -1/h^2 & & \\ & \ddots & \ddots & \ddots & \\ & & -1/h^2 & 1+2/h^2 & -1/h^2 \\ & & & -1/h^2 & 1+1/h^2 \end{pmatrix}$$

where h is the step size of the difference grid.

Suppose Eq. (9) is already a discrete matrix–vector equation. We find that Eq. (9) can be easily solved since the coefficient matrix $L^*L + \alpha H$ is positive definite for some $\alpha > 0$. Note that this kind of choice of the regularization parameter is not optimal. Practically, the regularization parameter α is closely related with the noise level. Therefore, we apply the parameter choice method developed in Ref. [10], i.e., the optimized parameter α^* is the root of the following nonlinear equation:

$$\Psi(\alpha) = \|Lg_\alpha - I\|^2_{L_2} - \delta^2 \tag{10}$$

where δ is the noise level in $(0, 1)$.

It is easy to show that $\Psi(\alpha)$ is differentiable. Therefore, fast algorithms for solving α^* can be implemented, say cubic convergent algorithm developed in Ref. [10]

$$\alpha_{k+1} = \alpha_k - \frac{2\Psi(\alpha_k)}{\Psi'(\alpha_k) + (\Psi'(\alpha_k)^2 - 2\Psi(\alpha_k)\Psi''(\alpha_k))^{1/2}} \tag{11}$$

Denoting by $\beta(\alpha) = \|g_\alpha\|^2$, we have

$$\Psi'(\alpha) = -\alpha\beta'(\alpha),$$

$$\Psi''(\alpha) = -\beta'(\alpha) - 2\alpha\left[\left\|\frac{\mathrm{d}g_\alpha}{\mathrm{d}\alpha}\right\|^2 + \left(g_\alpha, \frac{\mathrm{d}^2 g_\alpha}{\mathrm{d}\alpha^2}\right)\right]$$

Finding g_α, $\mathrm{d}g_\alpha/\mathrm{d}\alpha$, $\mathrm{d}^2 g_\alpha/\mathrm{d}\alpha^2$ will lead to solve the following equations:

$$(A^{\mathrm{T}}A + \alpha H) g_{\alpha_k} = A^{\mathrm{T}} I \tag{12}$$

$$(A^{\mathrm{T}}A + \alpha H) g'_{\alpha_k} = -Hg_{\alpha_k} \tag{13}$$

$$(A^{T}A + \alpha H) g''_{\alpha_k} = -2Hg'_{\alpha_k}. \tag{14}$$

For the solution of the linear matrix–vector equations (12)–(14), we use the Cholesky decomposition method. A remarkable characteristic of the solution of (12)–(14) is that the Cholesky decomposition of the coefficient matrix $A^{\mathrm{T}}A + \alpha H$ needs only once, then the three vectors $g_\alpha, \mathrm{d}g_\alpha/\mathrm{d}\alpha$, $\mathrm{d}^2 g_\alpha/\mathrm{d}\alpha^2$ can be obtained cheaply.

4. Numerical theoretical simulation

In order to testify the stability and reliability of the algorithm we generated a theoretical spectral distribution, which is shown in Fig. 3b, according to the parameters of 4W1A beamline in BSRF. The energy range of the object distribution is from 4 to 30 keV. The material for attenuation is Al whose thickness was chosen from 0 to 10 mm and the absorption coefficients were quoted from Ref. [11]. Fig. 3a shows the attenuation curve without noise and Fig. 3b shows the object spectrum.

Applying the algorithm to the attenuation curve without noise we get the numerical inversion results. In Fig. 3b, the solid line is the object spectrum and the circles are the numerical inversion results. The errors between the object and the results is shown in Fig. 4. The error level is less than 0.5%. It means that the algorithm is successful when the data have no noise.

In order to test the antinoise capability of the algorithm, a Gaussian random white noise was added to the simulated attenuation curve. In one situation, the random noise level in $[-0.1, 0.1]$ is added, and another one in $[-1, 1]$. Fig. 5a

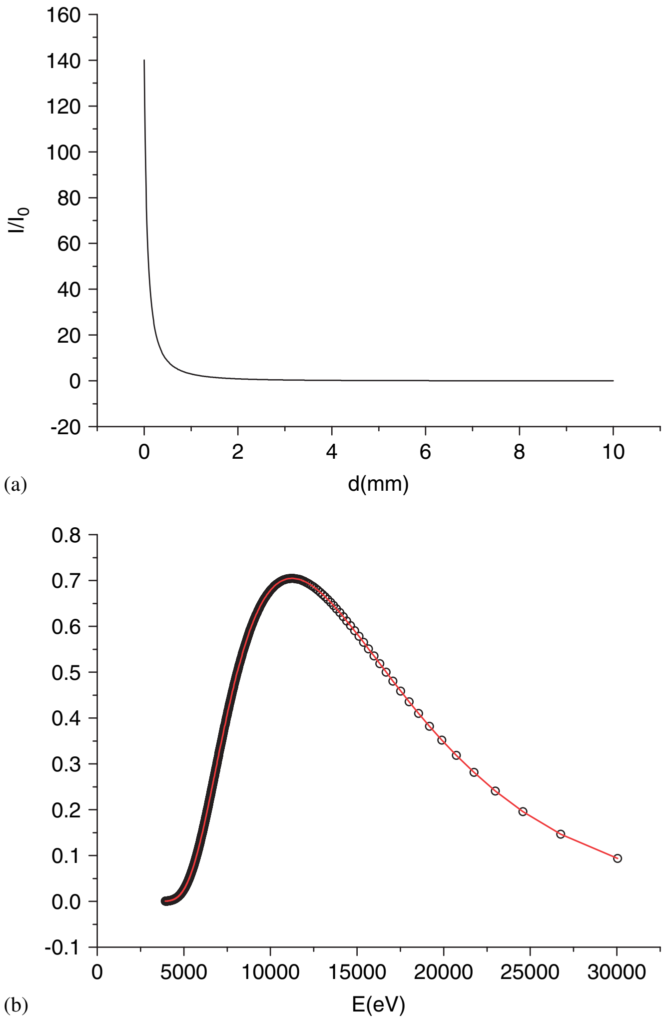

Fig. 3. (a) The simulated attenuation curve without noise; (b) the solid line is the object distribution. The circles are the numerical inversion results from the simulated attenuation data without noise.

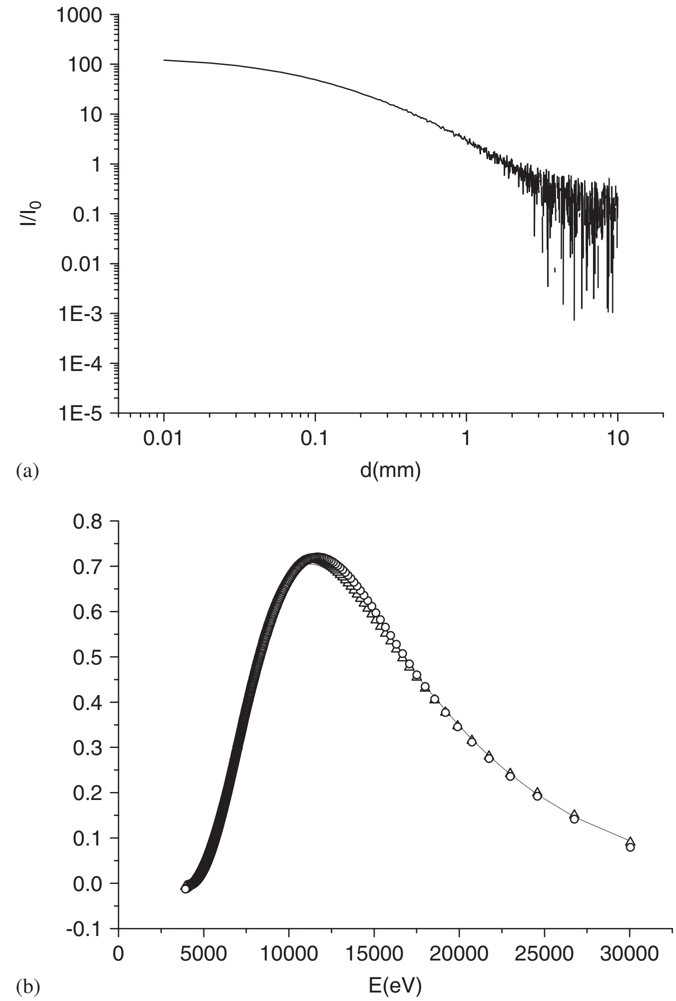

Fig. 5. (a) The curve added Gaussian random white-noise level in $[-1, 1]$. In (b), the solid line is the object distribution. The triangles are the numerical inversion results of the attenuation curves with Gaussian random white noise level in $[-0.1, 0.1]$ and the circles are those in level $[-1, 1]$.

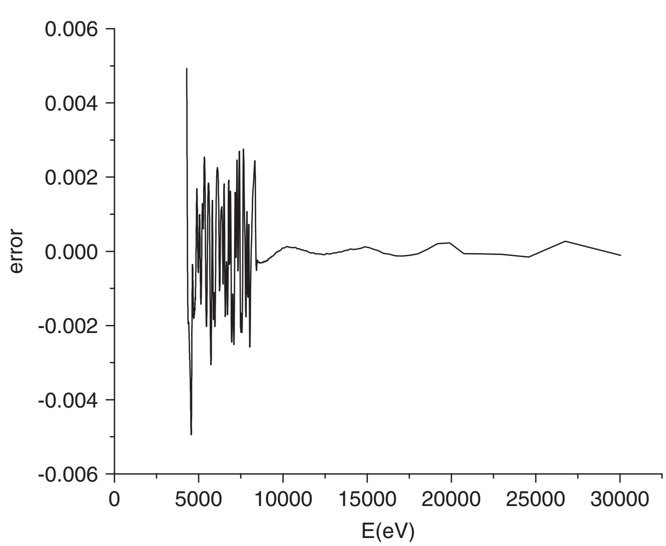

Fig. 4. The relative error between the object spectrum and the numerical inversion results from the simulated attenuation data without noise.

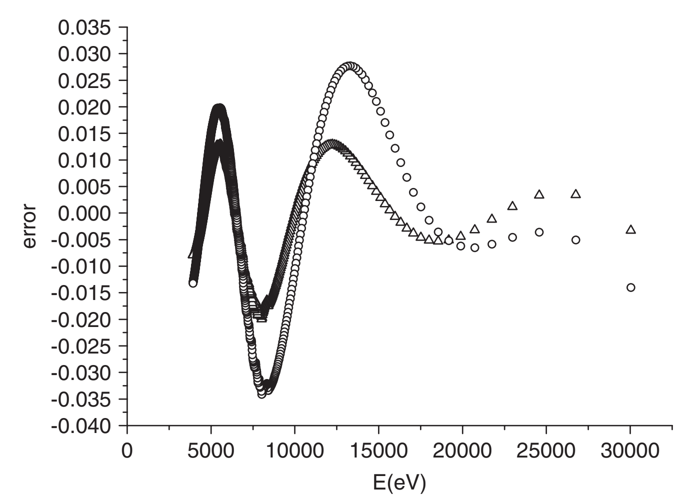

Fig. 6. The triangles are the error between the object distribution and the numerical inversion results from the simulated attenuation data with Gaussian random white-noise level in $[-0.1, 0.1]$ and the circles are those in $[-1, 1]$.

shows the results after adding noise. The effects of the noise to the simulated attenuation curve can be seen clearly in the partial enlarged detail.

The numerical inversion results of the two curves with noise are shown in Fig. 5b. The errors between the true and the computational results are shown in Fig. 6. It indicates that the numerical inversion results and the object distribution are very similar. The noise increases 9 times but the errors between the true and the numerical inversion results increase only one time. This shows that the algorithm is stable and reliable.

5. Results and discussion

All experiments were done at 4W1B beamline in BSRF. In our experiments the thickness of the tip of the filtration is about 0.25 mm. It means that SR will be absorbed by an Al foil of 0.25 mm before we measure it. Therefore, in numerical comparison with the theoretical values, an 0.25-mm-thick Al is added. As is pointed out in the above section, all of the constants involved in computation are omitted. Moreover, all of the curves are normalized by the maximum.

In our calculation, 1000 points were chosen from the measurements. The inversion results are shown in Fig. 7. The circles represent the numerical inversion results from experiment data. The dash line denotes the theoretical distribution of the light in the center of the cross-section. The solid line represents the theoretical distribution after considering that the beamline direction is offset from source central direction by 16.7 mrad. Compared with theoretical results and the calculation results, it is obvious that the circles are more similar to the solid line. It is consistent basically with the installation of 4W1B beamline which has 12–15 mrad horizontal departure. We can draw a conclusion that the beam position of the 4W1 is offset from source central direction by 16.7 mrad due to the change of electron orbit.

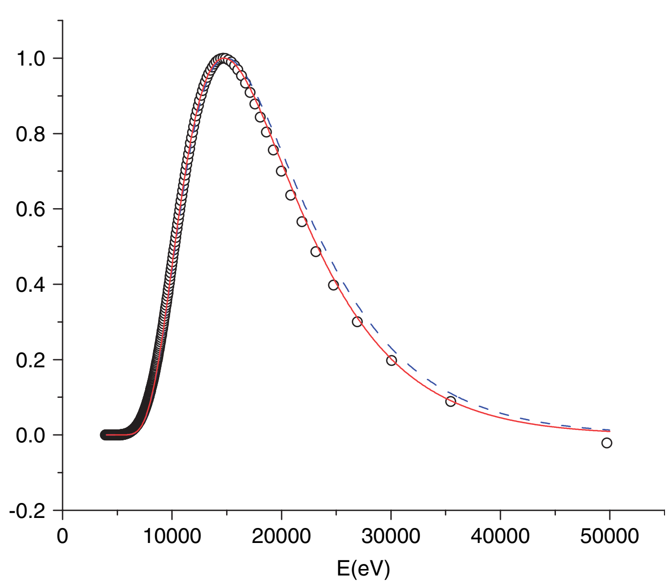

Fig. 7. The circles are the numerical inversion results from experiment data. The dash line is the theoretical distribution of the center of the light. The solid line represents the theoretical distribution after considering the beamline direction is offset from source central direction by 16.7 mrad.

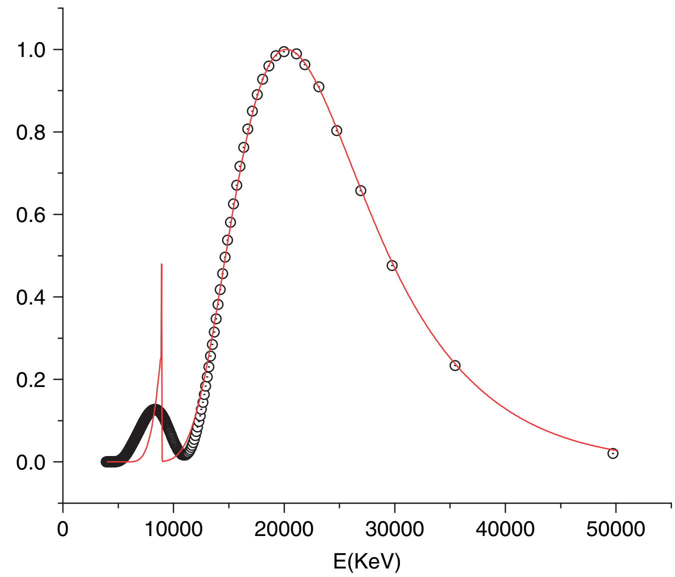

Fig. 8. The solid line is the theoretical result of the white light absorbed by Cu. The circles are the numerical inversion results. The position of Cu absorption peak has an error level of 6%.

In order to check the reliability of the inversion algorithm, we have collected the data with 35 μm Cu in the light path. The spectrum with Cu absorption was reconstructed by same algorithm. The result is shown in Fig. 8. The solid line is the theoretical result of the white light absorbed by Cu and the circles are the numerical inversion results. We can clearly see that the position of the absorption edge of Cu can be reconstructed. It proves that the numerical results of the spectrum absorbed by Cu are reliable. Furthermore, it proves that the numerical results of white light are reliable.

We can see that the method is successful to measure the spectrum of SR. However, some problems are still in existence. The first problem is that the tip of the filtration is too thick. The spectrum below 10 keV is attenuated too much, which can be seen in Fig. 7. In order to rebuild the spectrum of low energy, we need to reduce the thickness of the tip as much as possible and choose some kind of materials with low absorption instead of Al. The second problem is that the calculated Cu absorption edge is not sharp enough (see Fig. 8). In order to get a sharp absorption edge we have to do more work on the algorithm.

6. Conclusion and discussion

The current paper has described a simple experimental method and a reliable algorithm to measure and reconstruct the spectrum of SR. The inversion algorithm was tested by theoretical spectral distribution. Several practical measurements were carried out at 4W1B beamline in BSRF, and the numerical results can be proved to be reliable. Facing with such an ill-posed problem, Tikhonov regularization method exhibits good stability.

The stable algorithm and plenty of experimental data ensure the reliability of reconstructed spectrum. This method can be used to measure the spectrum of X-ray.

Acknowledgment

The authors are very grateful to Professor Dashi Li, Dr. Longhua Jiang, Dr. Jia-ou Wang, Caihao Hong and Wangsheng Chu for discussions.

References

[1] L. Silverstein, J. Opt. Soc. Am. 22 (1932) 265.
[2] G.E. Bell, Br. J. Radiol. 9 (1936) 680.
[3] J.R. Greening, Br. J. Radiol. 36 (1963) 363.
[4] J.W. Twidell, Phys. Med. Biol. 15 (1970) 529.
[5] B.W. Soole, Phys. Med. Biol. 21 (1976) 369.
[6] S. Tominaga, Nucl. Instr. and Meth. A 192 (1982) 415.
[7] H.M. Kramer, H. Von Seggern, Nucl. Instr. and Meth. A 213 (1983) 373.
[8] S. Tominaga, Nucl. Instr. and Meth. A 243 (1986) 530.
[9] T.Y. Xiao, S.G. Yu, Y.F. Wang, Numerical Methods for Inverse Problems, Science Press, Beijing, 2003.
[10] Y.F. Wang, T.Y. Xiao, Inverse Problems 17 (2001) 281.
[11] C.T. Chantler, J. Phys. Chem. Ref. Data 24 (1995) 71.